

The Berezinskii-Kosterlitz-Thouless Transition

Lara Turgut Francesco Conoscenti Ben Bullinger

Computational Statistical Physics (402-0812-00L), Spring 2025

Outline

1. Introduction
2. Theoretical Background
3. Monte Carlo Methods
4. Thermodynamic Observables
5. Estimating $T_{KT}(L)$
6. Implementation Details & Error Analysis
7. Results and Analysis
8. Conclusion

Outline

1. Introduction

2. Theoretical Background

3. Monte Carlo Methods

4. Thermodynamic Observables

5. Estimating $T_{KT}(L)$

6. Implementation Details & Error Analysis

7. Results and Analysis

8. Conclusion

The 2D XY Model

XY model: classical continuous spins on a 2D lattice, with $O(2)$ symmetry.

$$H = -J \sum_{\langle i,j \rangle} \mathbf{S}_i \cdot \mathbf{S}_j = -J \sum_{\langle i,j \rangle} \cos(\theta_i - \theta_j)$$

Each spin is a unit vector $\mathbf{S}_i = (\cos \theta_i, \sin \theta_i)$.

- ▶ **Mermin-Wagner theorem:** No spontaneous breaking of continuous symmetries at $T > 0$ in $d \leq 2$.
- ▶ Yet, the 2D XY model *does* exhibit a phase transition!
- ▶ The Berezinskii-Kosterlitz-Thouless (BKT) transition:
 - ▶ Topological phase transition
 - ▶ Infinite order transition, with no conventional order parameter.

Outline

1. Introduction
- 2. Theoretical Background**
3. Monte Carlo Methods
4. Thermodynamic Observables
5. Estimating $T_{KT}(L)$
6. Implementation Details & Error Analysis
7. Results and Analysis
8. Conclusion

Order in the 2D XY Model

Hamiltonian Low Temperature expansion:

- Second order Taylor expansion $\cos(\theta_i - \theta_j) \rightarrow 1 - \frac{1}{2}(\theta_i - \theta_j)^2$
- Continuum limit $\theta_i \rightarrow \theta(\mathbf{r})$, $\theta_i - \theta_j \rightarrow \nabla\theta(\mathbf{r})$

$$H \approx E_0 + \frac{J}{2} \int d\mathbf{r} (\nabla\theta(\mathbf{r}))^2$$

Correlation function analysis

$$g(r) = \langle e^{i(\theta(\mathbf{r}) - \theta(0))} \rangle$$

- **Low-T phase (QLRO)** [1]: $g(r) \sim r^{-\eta(T)}$, Algebraic decay of correlations, $\xi = \infty$.
- **High-T phase (Disordered)**: $g(r) \sim e^{-r/\xi(T)}$, Exponential decay.

Vortices

Steady states of this Hamiltonian are[1]:

$$\frac{\delta H}{\delta \theta} = 0 \Rightarrow \nabla^2 \theta = 0$$

This Laplace equation has 2 types of solutions

- ▶ **Ground state:** $\theta(r) = \text{const}$ with Ferromagnetic order, $E = 0$
- ▶ **Vortices:** topological defects with winding of $2\pi n$ [1]

$$\oint_{r_0} \nabla \theta \cdot d\mathbf{l} = 2\pi n$$

Energy difference of adding a single vortex is:

$$\Delta E = E_{\text{vort}} - E_{\text{no_vort}} = \pi J \int \frac{d\mathbf{r}}{r} = \pi J \ln \frac{L}{a}$$

Entropy of a single vortex:

$$\Delta S = k_B \ln \frac{L^2}{a^2} = 2k_B \ln \frac{L}{a}$$

Identify the Phases

The Free energy of a single vortex is

$$\Delta F = \Delta E - T\Delta S = (\pi J - 2k_B T) \ln \frac{L}{a}$$

It identify 2 different **phases**:

- ▶ For $T > \frac{\pi J}{2k_B}$: $\Delta F < 0$ free vortices proliferate ($\Delta F \rightarrow -\infty$ as $L \rightarrow \infty$)
- ▶ For $T < \frac{\pi J}{2k_B}$: $\Delta F > 0$, single vortices are forbidden ($\Delta F \rightarrow \infty$ as $L \rightarrow \infty$)

But pairs of a vortex and an antivortex can appear.

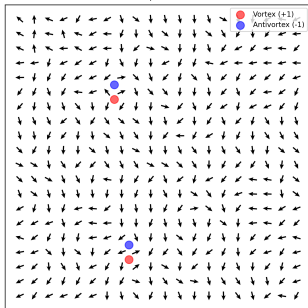
$$\Delta F_{pair} = (\pi J - 2k_B T) \ln \frac{r}{a}$$

Pairs are stable because their energy is finite and entropy is insufficient to unbind them.

Visualizing Spin Configurations and Vortices

QLRO

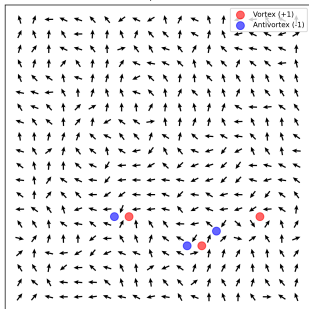
XY Model Spin Configuration
 $L = 20, T = 0.85$



$$T = 0.85 \lesssim T_{KT}$$

Transition

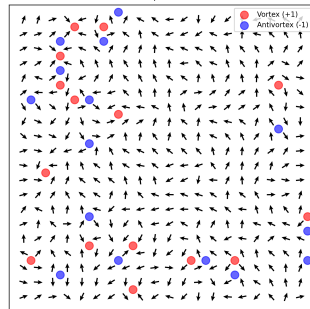
XY Model Spin Configuration
 $L = 20, T = 0.92$



$$T \approx 0.92 \gtrsim T_{KT}$$

Disorder

XY Model Spin Configuration
 $L = 20, T = 1.20$



$$T = 1.20 > T_{KT}$$

Renormalization Group

Understand large-scale behavior by tracking how coupling constants evolve with scale.

- **Mapping** the 2D XY model to a 2D Coulomb gas.

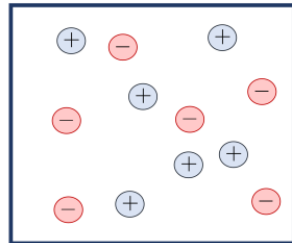
Topological Hamiltonian:

$$H_v = \sum_i H_{n_i}^{\text{core}} + 2\pi K \sum_{i < j} n_i n_j \ln(|r_i - r_j|)$$

Fugacity: $y_0 = \exp(H_{n_i}^{\text{core}})$ regulates vortex excitation.

- **Screening** modifies the effective interaction:

$$H_{\text{eff}}(r - r') \approx -2\pi K_{\text{eff}} \ln(r - r')$$

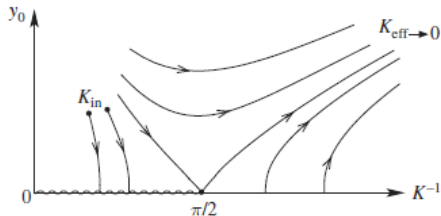


Partition function of XY Model resembles that of a neutral 2D Coulomb gas

Renormalization Group

► RG Flow equations:[1]

$$\begin{cases} \frac{dK^{-1}}{dl} = 4\pi^3 y_0^2 + \mathcal{O}(y_0^4), \\ \frac{dy_0}{dl} = (2 - \pi K) y_0 + \mathcal{O}(y_0^3) \end{cases}$$



Universal jump:

$$\lim_{l \rightarrow \infty} K^{-1}(T_{KT}^-) = \pi/2,$$

$$\lim_{l \rightarrow \infty} K^{-1}(T > T_{KT}) = 0$$

- $y_0 = 0$ is a line of fixed points up to $K^{-1} = \pi/2$
- Below T_{KT} : bound vortex pairs (quasi-ordered)
- Above T_{KT} : unbound vortices (disordered)

Outline

1. Introduction
2. Theoretical Background
- 3. Monte Carlo Methods**
4. Thermodynamic Observables
5. Estimating $T_{KT}(L)$
6. Implementation Details & Error Analysis
7. Results and Analysis
8. Conclusion

Simulating the XY Model

- ▶ **Challenges** in simulating BKT transition:
 - ▶ Critical slowing down near phase transition
 - ▶ Need for large system sizes (finite-size effects)
 - ▶ Long correlation times

Simulating the XY Model

- ▶ **Challenges** in simulating BKT transition:
 - ▶ Critical slowing down near phase transition
 - ▶ Need for large system sizes (finite-size effects)
 - ▶ Long correlation times
- ▶ **Metropolis algorithm:**

- ▶ Energy change for spin flip

$$\Delta E = -J \sum_{\langle i,j \rangle} [\cos(\theta'_i - \theta_j) - \cos(\theta_i - \theta_j)]$$

- ▶ Accept new state with probability

$$\mathbb{P}_{\text{accept}} = \min(1, e^{-\beta \Delta E})$$

- ▶ **Very inefficient near critical point** due to large correlated regions

Simulating the XY Model

- ▶ **Challenges** in simulating BKT transition:
 - ▶ Critical slowing down near phase transition
 - ▶ Need for large system sizes (finite-size effects)
 - ▶ Long correlation times
- ▶ **Metropolis algorithm:**
 - ▶ Energy change for spin flip

$$\Delta E = -J \sum_{\langle i,j \rangle} [\cos(\theta'_i - \theta_j) - \cos(\theta_i - \theta_j)]$$

- ▶ Accept new state with probability

$$\mathbb{P}_{\text{accept}} = \min(1, e^{-\beta \Delta E})$$

- ▶ **Very inefficient near critical point** due to large correlated regions
- ▶ **Wolff cluster algorithm:**
 - ▶ Updates entire clusters of spins, **significantly reducing critical slowing down.**

Wolff Cluster Algorithm for the XY Model

Algorithm [1]:

- ▶ **Choose a random reflection axis:** Pick an angle $\phi \in [0, 2\pi)$ and define the unit vector $\mathbf{r} = (\cos \phi, \sin \phi)$.
- ▶ **Project spins:** For each site i , compute $s_i = \mathbf{S}_i \cdot \mathbf{r} = \cos(\theta_i - \phi)$.
- ▶ **Cluster growth:**
 - ▶ Pick a random seed site i_0 .
 - ▶ For each neighbor j of a site i in the cluster, add j to the cluster with probability:

$$\mathbb{P}_{\text{add}} = 1 - \exp[\min(0, -2\beta J s_i s_j)]$$

- ▶ **Reflect all spins in the cluster:** $\theta_i \rightarrow 2\phi - \theta_i \quad \forall i \in \text{cluster}$.

Wolff Cluster Algorithm for the XY Model

Algorithm [1]:

- ▶ **Choose a random reflection axis:** Pick an angle $\phi \in [0, 2\pi)$ and define the unit vector $\mathbf{r} = (\cos \phi, \sin \phi)$.
- ▶ **Project spins:** For each site i , compute $s_i = \mathbf{S}_i \cdot \mathbf{r} = \cos(\theta_i - \phi)$.
- ▶ **Cluster growth:**
 - ▶ Pick a random seed site i_0 .
 - ▶ For each neighbor j of a site i in the cluster, add j to the cluster with probability:

$$\mathbb{P}_{\text{add}} = 1 - \exp[\min(0, -2\beta J s_i s_j)]$$

- ▶ **Reflect all spins in the cluster:** $\theta_i \rightarrow 2\phi - \theta_i \quad \forall i \in \text{cluster}.$

Remarks

- ▶ Non-local updates **reduce autocorrelation times** compared to Metropolis algorithm
- ▶ Dramatically **reduces critical slowing down** near T_{KT} by building clusters that scale with correlation length $\xi(T)$

Outline

1. Introduction
2. Theoretical Background
3. Monte Carlo Methods
- 4. Thermodynamic Observables**
5. Estimating $T_{KT}(L)$
6. Implementation Details & Error Analysis
7. Results and Analysis
8. Conclusion

Thermodynamic Observables

Observable	Formula
Energy per spin	$e = \langle H \rangle / N$
Magnetization	$\langle \mathbf{m} \rangle$
Specific heat	$c_v = \frac{\langle E^2 \rangle - \langle E \rangle^2}{NT^2}$
Susceptibility	$\chi = \frac{N}{T} (\langle \mathbf{m} ^2 \rangle - \langle \mathbf{m} \rangle^2)$
Spin stiffness (for $J = 1$)	$\rho_s = \frac{1}{2N} \left(\left\langle \sum_{\langle i,j \rangle_x} \cos(\Delta\theta_{ij}) \right\rangle - \beta \left\langle \left(\sum_{\langle i,j \rangle_x} \sin(\Delta\theta_{ij}) \right)^2 \right\rangle \right) + (x \leftrightarrow y)$
Vortex density (ω_v)	$\omega_v = \left\langle \frac{1}{N} \sum_{\square} \left \frac{1}{2\pi} \oint_{\square} d\theta \right \right\rangle$
Correlation function	$g(r) = \langle e^{i(\theta(\mathbf{r}) - \theta(0))} \rangle$

Thermodynamic Observables

Observable	Formula
Energy per spin	$e = \langle H \rangle / N$
Magnetization	$\langle \mathbf{m} \rangle$
Specific heat	$c_v = \frac{\langle E^2 \rangle - \langle E \rangle^2}{NT^2}$
Susceptibility	$\chi = \frac{N}{T} (\langle \mathbf{m} ^2 \rangle - \langle \mathbf{m} \rangle^2)$
Spin stiffness (for $J = 1$)	$\rho_s = \frac{1}{2N} \left(\left\langle \sum_{\langle i,j \rangle_x} \cos(\Delta\theta_{ij}) \right\rangle - \beta \left\langle \left(\sum_{\langle i,j \rangle_x} \sin(\Delta\theta_{ij}) \right)^2 \right\rangle \right) + (x \leftrightarrow y)$
Vortex density (ω_v)	$\omega_v = \left\langle \frac{1}{N} \sum_{\square} \left \frac{1}{2\pi} \oint_{\square} d\theta \right \right\rangle$
Correlation function	$g(r) = \langle e^{i(\theta(\mathbf{r}) - \theta(0))} \rangle$

The spin stiffness and correlation function are used to locate T_{KT}

Outline

1. Introduction
2. Theoretical Background
3. Monte Carlo Methods
4. Thermodynamic Observables
- 5. Estimating $T_{KT}(L)$**
6. Implementation Details & Error Analysis
7. Results and Analysis
8. Conclusion

Estimating $T_{KT}(L)$

Estimating $T_{KT}(L)$

- **Stiffness:** The estimate $T_{KT}^{\rho_s}$ is extracted by intersecting $\rho_s(T)$ with the **Nelson-Kosterlitz Jump** line [5]:

$$\rho_s(T) = \frac{2k_B T_{KT}}{\pi}$$

Estimating $T_{KT}(L)$

- **Stiffness:** The estimate $T_{KT}^{\rho_s}$ is extracted by intersecting $\rho_s(T)$ with the **Nelson-Kosterlitz Jump** line [5]:

$$\rho_s(T) = \frac{2k_B T_{KT}}{\pi}$$

- **Correlation decay exponent:** The decay exponent η is extracted by fitting the correlation function $g(r) \sim r^{-\eta}$ in the QLRO regime. Intersecting $\eta(T)$ with the **universal value** [3]

$$\eta = 1/4$$

yields the estimate $T_{KT}^{\eta}(L)$.

Estimating $T_{KT}(L)$

- **Stiffness:** The estimate $T_{KT}^{\rho_s}$ is extracted by intersecting $\rho_s(T)$ with the **Nelson-Kosterlitz Jump** line [5]:

$$\rho_s(T) = \frac{2k_B T_{KT}}{\pi}$$

- **Correlation decay exponent:** The decay exponent η is extracted by fitting the correlation function $g(r) \sim r^{-\eta}$ in the QLRO regime. Intersecting $\eta(T)$ with the **universal value** [3]

$$\eta = 1/4$$

yields the estimate $T_{KT}^{\eta}(L)$.

- **Correlation length:** The correlation length ξ is extracted by fitting the correlation function $g(r) \sim e^{-r/\xi(T)}$ in the disordered regime, where for $T \rightarrow T_{BKT}^+$, ξ **diverges exponentially** in the thermodynamic limit [1]:

$$\xi(T) \approx a \exp \left[\frac{\pi^2}{8b} \sqrt{\frac{T_{KT}}{T - T_{KT}}} \right]$$

This fit yields $T_{KT}^{\xi}(L)$.

Outline

1. Introduction
2. Theoretical Background
3. Monte Carlo Methods
4. Thermodynamic Observables
5. Estimating $T_{KT}(L)$
- 6. Implementation Details & Error Analysis**
7. Results and Analysis
8. Conclusion

Implementation Details

- ▶ Simulation structure:
 - ▶ **Thermalization:** Ensure equilibrium is reached at each target temperature.
 - ▶ **Measurement:** Measure observables over many sweeps in equilibrium.
 - ▶ **Analysis:** Calculate averages, estimate $T_{KT}(L)$, perform **finite-size scaling analysis** to extract $T_{KT}(\infty)$

Implementation Details

- ▶ Simulation structure:
 - ▶ **Thermalization**: Ensure equilibrium is reached at each target temperature.
 - ▶ **Measurement**: Measure observables over many sweeps in equilibrium.
 - ▶ **Analysis**: Calculate averages, estimate $T_{KT}(L)$, perform **finite-size scaling analysis** to extract $T_{KT}(\infty)$
- ▶ Optimizations:
 - ▶ Pre-computation of neighbor indices.
 - ▶ Vectorization of NumPy operations.
 - ▶ **Just-in-time compilation** (Numba '@njit' [4]) for core simulation loops (Wolff/Metropolis updates, energy calculations, observable measurements).
 - ▶ **Parallelization** over (L, T) pairs

Error Analysis: Estimating Statistical Uncertainty

We use the **standard error** for sufficiently decorrelated data, and **Jackknife resampling** otherwise.

Error Analysis: Estimating Statistical Uncertainty

We use the **standard error** for sufficiently decorrelated data, and **Jackknife resampling** otherwise.

- ▶ **Standard Error of the Mean (SEM):**

- ▶ Formula: $SE = s / \sqrt{N_{\text{meas}}}$ (where s is the sample standard deviation).
- ▶ L^2 cluster attempts per Wolff sweep significantly decorrelate direct measurement data
- ▶ Used for: **Energy** and **Magnetization**.

Error Analysis: Estimating Statistical Uncertainty

We use the **standard error** for sufficiently decorrelated data, and **Jackknife resampling** otherwise.

► Standard Error of the Mean (SEM):

- Formula: $SE = s/\sqrt{N_{\text{meas}}}$ (where s is the sample standard deviation).
- L^2 cluster attempts per Wolff sweep significantly decorrelate direct measurement data
- Used for: **Energy** and **Magnetization**.

► Jackknife Resampling:

- Recalculate statistics on N_{meas} subsamples obtained in leave-one-out manner

$$\sigma_{\text{JK}}^2 = \frac{N_{\text{meas}} - 1}{N_{\text{meas}}} \sum_{i=1}^{N_{\text{meas}}} (\bar{O}_i - \bar{O})^2$$

where \bar{O}_i is the statistic with the i -th observation removed, and \bar{O} is the average of the \bar{O}_i .

- The variance of the jackknife estimates provides an estimate of the true variance.
- Convenient for non-linear functions of measured quantities and for correlated data.
- Used for: **Spin Stiffness**, **Susceptibility**, **Specific Heat**, **Binder Cumulant**, **Vortex Density**, **η exponent**, and **Correlation length ξ** .

Error Analysis

Error Propagation for Derived Critical Temperatures

- ▶ To estimate the errors on $T_{KT}(L)$ we
 - ▶ directly propagate the errors on the primary observables
 - ▶ propagate the covariance matrix of intermediate fits (in the case of $\xi(T)$)

Error Analysis

Error Propagation for Derived Critical Temperatures

- ▶ To estimate the errors on $T_{KT}(L)$ we
 - ▶ directly propagate the errors on the primary observables
 - ▶ propagate the covariance matrix of intermediate fits (in the case of $\xi(T)$)
- ▶ Obtain $T_{KT}(\infty)$ by **weighted linear regression** on the scaling form

$$T_{KT}(L) = T_{KT}(\infty) + \frac{a}{(\ln L)^2}$$

with weights $1/\sigma_{T_{KT}(L)}^2$ (where $\sigma_{T_{KT}(L)}$ is the standard error on each $T_{KT}(L)$).

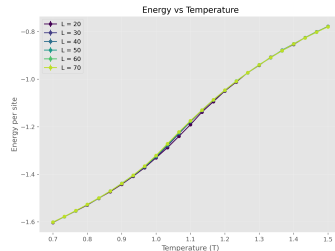
Outline

1. Introduction
2. Theoretical Background
3. Monte Carlo Methods
4. Thermodynamic Observables
5. Estimating $T_{KT}(L)$
6. Implementation Details & Error Analysis
- 7. Results and Analysis**
8. Conclusion

Energy and Specific Heat

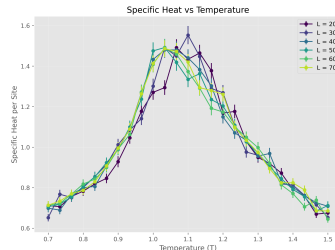
Energy per Spin (e)

- Increases smoothly and monotonically with temperature, no sharp change in slope near the transition.



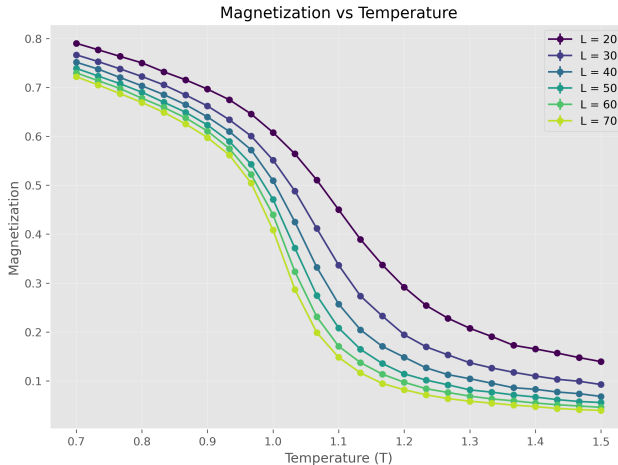
Specific Heat (c_v)

- Exhibits a broad peak around $T \approx 1.1 J/k_B$.
- No divergence at T_{KT} .



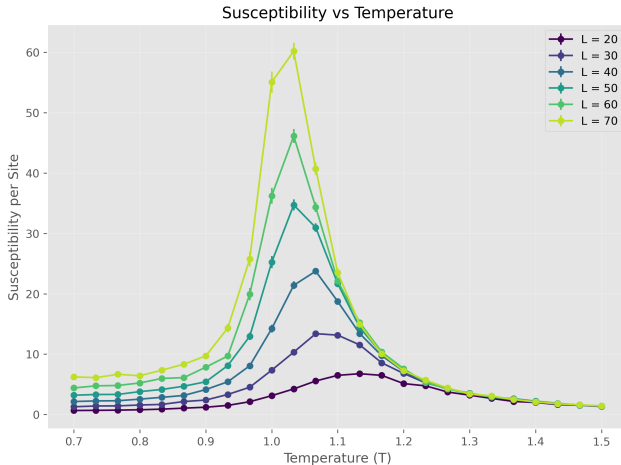
Magnetization ($|\mathbf{m}|$)

- ▶ Decreases with L , consistent with the **Mermin–Wagner theorem**.
- ▶ Decays slowly with L in the low-temperature phase, consistent with QLRO: $|\mathbf{m}| \sim L^{-\eta(T)/2}$. [2]
- ▶ Decays rapidly with L in the high-temperature disordered phase. [2]



Susceptibility (χ)

- ▶ Peaks in the range
 $T \approx 1.0\text{--}1.1 J/k_B$
- ▶ **The peak height increases significantly with L** , as the correlation function decays algebraically in the $T < T_{\text{BKT}}$ phase: $G(r) \sim r^{-\eta(T)}$, leading to a susceptibility that scales as $\chi \sim L^{2-\eta(T)}$ [3].
- ▶ χ diverges as $L \rightarrow \infty$ for $T \leq T_{\text{KT}}$.
- ▶ For $T > T_{\text{KT}}$, exponential decay $G(r) \sim e^{-r/\xi}$ implies $\chi \sim \xi^2(T)$, so χ stays finite as $L \rightarrow \infty$. [3]



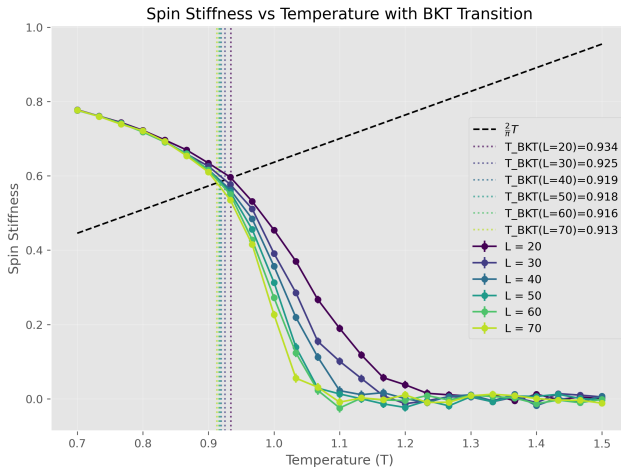
Spin Stiffness (Helicity Modulus ρ_s)

- ▶ Smooth curves due to finite sized systems.

- ▶ **Universal jump** prediction by Nelson-Kosterlitz:

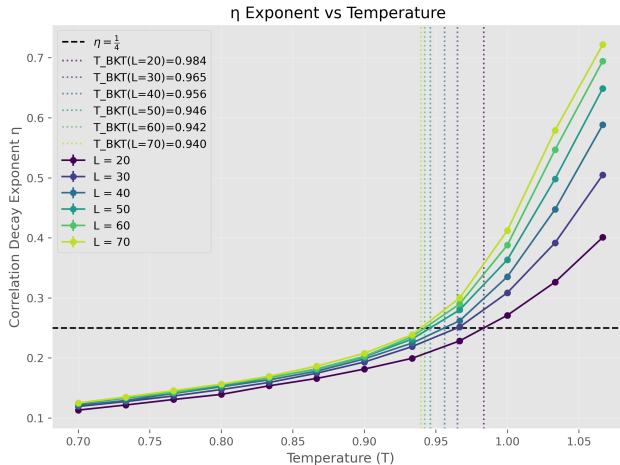
$$\rho_s(T_{KT}^-) = \frac{2k_B T_{KT}}{\pi}$$

- ▶ Intersection of $\rho_s(T, L)$ with this line provides an estimate of $T_{KT}(L)$.
- ▶ For $L = 70$, our data suggests $T_{KT} \approx 0.913J/k_B$.



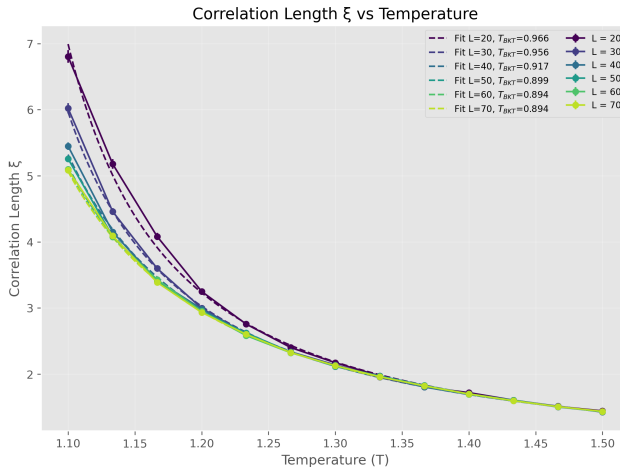
Decay exponent (η)

- ▶ The decay exponent η is extracted by fitting the spin–spin correlation function $G(r) \sim r^{-\eta}$.
- ▶ The dashed line indicates the **BKT transition criterion** $\eta = \frac{1}{4}$.
- ▶ The crossing points with the dashed line yield the estimates of T_{BKT} .
- ▶ For $L = 70$, our data suggests $T_{KT} \approx 0.940 J/k_B$.



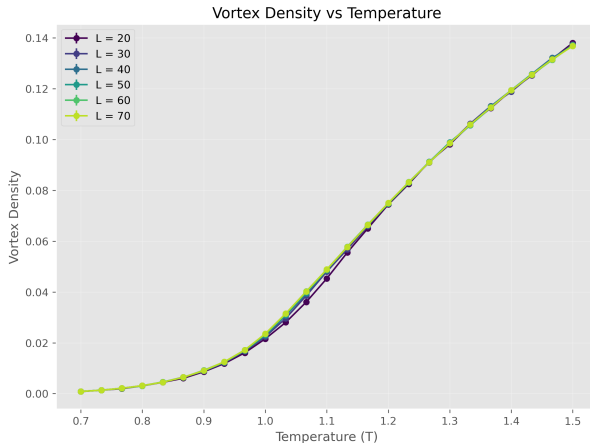
Correlation length (ξ)

- ▶ Rapid increase of ξ near the transition.
- ▶ As $T \rightarrow T_{KT}^+$, ξ diverges exponentially in the thermodynamic limit: $\xi(T) \propto \exp \left[\frac{\pi^2}{8b} \sqrt{\frac{T_{BKT}}{T - T_{BKT}}} \right]$, where b is a non-universal constant.
- ▶ For $L = 70$, our data suggests $T_{KT} \approx 0.894 J/k_B$.



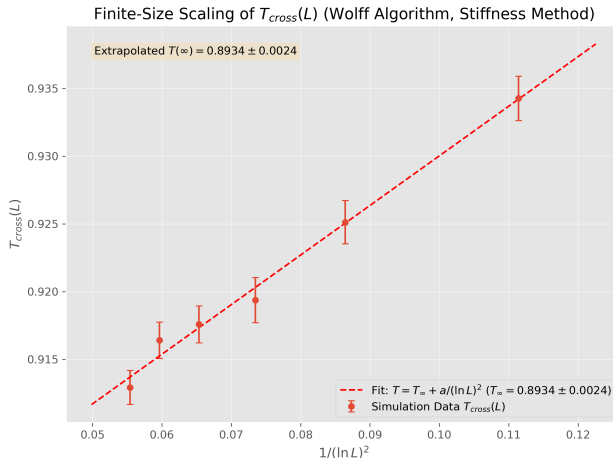
Vortex Density ω_v

- ▶ At low temperatures ($T \ll T_{KT}$):
 - ▶ Vortices exist only in tightly bound vortex-antivortex pairs.
 - ▶ Density is very low.
- ▶ Near T_{KT} :
 - ▶ Pairs start to unbind.
 - ▶ Density increases sharply.
- ▶ Above T_{KT} :
 - ▶ Proliferation of free vortices/antivortices.
 - ▶ Density becomes large, destroying QLRO.



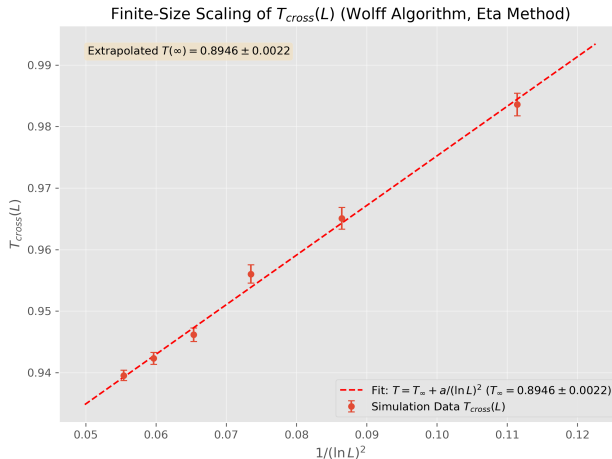
Finite-Size Scaling of $T_{KT}(L)$, Spin Stiffness Method

- ▶ Estimate $T_{KT}(L)$ for each size L from the intersection
 $\rho_s(T, L) = 2k_B T / \pi$.
- ▶ $T_{KT}(L) = T_{KT}(\infty) + \frac{a}{(\ln L)^2}$,
where a is non-universal constant.
- ▶ The y-intercept gives the estimate for $T_{KT}(\infty)$.
- ▶ Weighted linear fit yields:
 $T_{KT}(\infty) \approx 0.8934(24) J/k_B$
- ▶ Result is **consistent** with the literature value
 $T_{KT} \approx 0.89213(10) J/k_B$. [6]



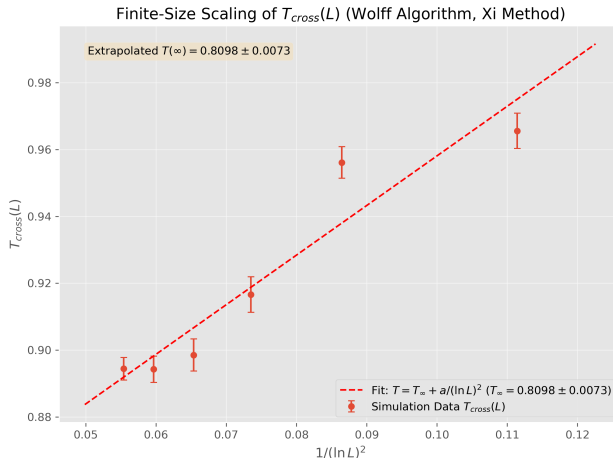
Finite-Size Scaling of $T_{KT}(L)$, η Method

- ▶ Estimate $T_{KT}(L)$ for each size L from the intersection $\eta(T, L) = 0.25$.
- ▶ $T_{KT}(L) = T_{KT}(\infty) + \frac{a}{(\ln L)^2}$, where a is non-universal constant.
- ▶ The y-intercept gives the estimate for $T_{KT}(\infty)$.
- ▶ Weighted linear fit yields:
 $T_{KT}(\infty) \approx 0.8946(22)J/k_B$
- ▶ Result is **nearly consistent** with the literature value
 $T_{KT} \approx 0.89213(10)J/k_B$. [6]



Finite-Size Scaling of $T_{KT}(L)$, ξ Method

- ▶ Estimate $T_{KT}(L)$ for each size L using $\xi(T) \propto \exp \left[\frac{\pi^2}{8b} \sqrt{\frac{T_{BKT}}{T - T_{BKT}}} \right]$.
- ▶ $T_{KT}(L) = T_{KT}(\infty) + \frac{a}{(\ln L)^2}$, where a is non-universal constant.
- ▶ The y-intercept gives the estimate for $T_{KT}(\infty)$.
- ▶ Weighted linear fit yields:
 $T_{KT}(\infty) \approx 0.8098(73) J/k_B$
- ▶ Result is **not consistent** with the literature value $T_{KT} \approx 0.89213(10) J/k_B$. [6]; possibly due to insufficient number of temperature points to reliably fit the exponential divergence of $\xi(T)$.



Outline

1. Introduction
2. Theoretical Background
3. Monte Carlo Methods
4. Thermodynamic Observables
5. Estimating $T_{KT}(L)$
6. Implementation Details & Error Analysis
7. Results and Analysis
- 8. Conclusion**

Conclusion

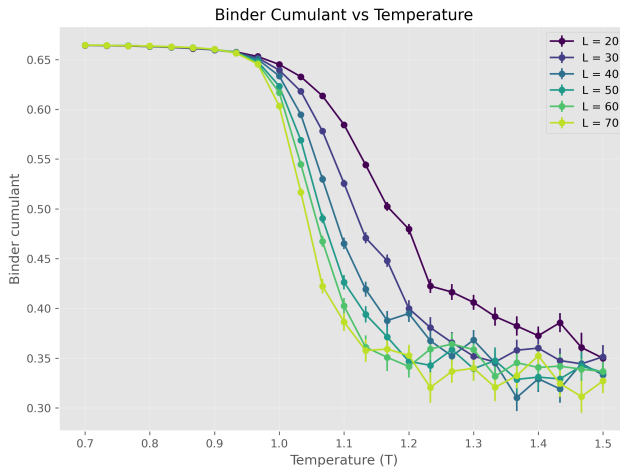
- ▶ Implemented the Wolff algorithm
- ▶ Measured observables for different system sizes
- ▶ Verified BKT transition and estimated $T_{KT} \approx 0.8934(24)J/k_B$

Thank you for your attention!


Back up slide I

Binder Cumulant $|U_L|$

- ▶ In the low-temperature phase, $|U_L|$ remains high and nearly size-independent.
- ▶ Around T_{BKT} , curves for different L start to separate.
- ▶ The absence of a common intersection point in the Binder cumulant curves indicates the lack of a conventional second-order phase transition.



References I

- [1] Victor Drouin-Touchette. “The kosterlitz-thouless phase transition: an introduction for the intrepid student”. In: *arXiv preprint arXiv:2207.13748* (2022).
- [2] Bhilahari Jeevanesan et al. “Emergent Power-Law Phase in the 2D Heisenberg Windmill Antiferromagnet: A Computational Experiment”. In: *Physical Review Letters* 115 (June 2015). doi: 10.1103/PhysRevLett.115.177201 .
- [3] J Michael Kosterlitz. “The critical properties of the two-dimensional xy model”. In: *Journal of Physics C: Solid State Physics* 7.6 (1974), p. 1046.
- [4] Siu Kwan Lam, Antoine Pitrou, and Stanley Seibert. “Numba: A llvm-based python jit compiler”. In: *Proceedings of the Second Workshop on the LLVM Compiler Infrastructure in HPC*. 2015, pp. 1–6.
- [5] David R Nelson and John Michael Kosterlitz. “Universal jump in the superfluid density of two-dimensional superfluids”. In: *Physical Review Letters* 39.19 (1977), p. 1201.

References II

- [6] [Peter Olsson](#). “Monte Carlo analysis of the two-dimensional XY model. II. Comparison with the Kosterlitz renormalization-group equations”. In: *Physical Review B* 52.6 (1995), p. 4526.

Lara Turgut

ETH Zurich, Department of Physics

lturgut@ethz.ch

Francesco Conoscenti

ETH Zurich, Department of Information Technology and Electrical Engineering

fconoscenti@ethz.ch

Ben Bullinger

ETH Zurich, Department of Computer Science

bben@ethz.ch